Thin-film metal catalyst for the production of multi-wall and single-wall carbon nanotubes

R. G. Lacerda,[a] K. B. K. Teo, A. S. Teh, M. H. Yang, S. H. Dalal, D. A. Jefferson,[b] J. H. Durrell,[c] N. L. Rupesinghe, D. Roy, G. A. J. Amaratunga, and W. I. Milne
Engineering Department, University of Cambridge, Cambridge, CB2 1PZ, United Kingdom

F. Wyczisk and P. Legagneux
Thales Research and Technology France, Domaine de Corbeville, 91404 Orsay, France

M. Chhowalla
Department of Ceramic and Materials Engineering, Rutgers University, Piscataway, New Jersey 08854

(Received 5 April 2004; accepted 26 July 2004)

We present a detailed study of the growth of multiwall and single-wall carbon nanotubes (SWCNTs) by chemical-vapor deposition using a thin-film triple metal (Al/Fe/Mo) catalyst. Using Nanoauger spectroscopy, a full map of the metals in the sample surface is constructed and their evolution followed at different deposition temperatures. During the formation of SWCNTs at high temperatures (~1000 °C), the initial iron layer (~1 nm) is transformed into nanosized particles at the surface. In addition, the Al layer also plays a critical role during the annealing process by being altered into Al_xO_y particles. These particles act as a suitable underlayer to stabilize the nanosized Fe catalyst for nanotube growth. We also show that it is possible to resolve SWCNTs by mapping the areal intensity of carbon KVV Auger electrons. © *2004 American Institute of Physics*.
[DOI: 10.1063/1.1794359]

I. INTRODUCTION

Carbon nanotubes are a potential building block for the next generation of electronics and hence are the subject of intensive research recently.[1] In the past few years, the growth techniques employed have progressed greatly. In particular, there has been a large effort put into producing single-wall carbon nanotubes (SWCNTs). This particular kind of tube has only one cylindrical wall and therefore is a natural nanometer-sized material for use in electronic applications.[2,3] Significantly, the way the single layer of graphene wraps around itself determines whether the nanotube will behave as a semiconductor or a metal. Single-wall carbon nanotubes can be prepared by techniques such as laser ablation and arc discharge. However, these techniques produce by-products such as amorphous carbon, graphitic particles, and multiwall carbon nanotubes (MWCNTs) in addition to the desired single-wall tubes. At the moment, there are several obstacles to overcome before the material can be applied in micro/nanoelectronic products. Problems such as controlling the nanotube chirality, which determines the semiconductor or metallic behavior, still need to be demonstrated. Some success has been achieved in controlling nanotube position on patterned structures.[4–6] This success is mainly attributed to the use of thermal chemical-vapor deposition (CVD) as the synthesis technique.[7,8] This deposition method uses hydrocarbon gases as the carbon source and has proven to be an effective technique to prepare clean and isolated single-wall carbon nanotubes.[9] It is well known that one of the key difficulties in producing single-wall carbon nanotubes is to create metal catalyst seeds with sizes in the order of 1–7 nm, because particles larger than that mostly produce multiwall carbon nanotubes.[10] Wet chemical methods help to solve this problem because it is possible to prepare nanometer-sized catalyst particles in solution; they are therefore commonly used for the growth of SWCNTs, especially by thermal chemical-vapor deposition.[7,8] It has also been demonstrated that the catalyst size is the determining factor for the diameter of SWCNTs.[11,12] The production of SWCNTs by using a wet catalyst is understandable because there is a predetermined dispersion of nanometer-sized catalyst particles.

Recently, thin-film catalyst layers have been successfully employed in the single-wall carbon nanotube growth.[13–17] In a recent work, we also demonstrated that by using a rapid growth method and a thin-film triple layer (Al+Fe+Mo) as the catalyst, one could deposit isolated SWCNTs without the presence of unwanted amorphous carbon.[9] This technique has several advantages. Firstly, it allows a reliable and an accurate patterning of the catalyst using lithographic techniques. Secondly, depositing the thin-film metal catalyst is scalable, reproducible, and can be performed using standard techniques such as sputtering and evaporation, techniques which are widely employed in microelectronic device production.

However, there is presently no clear growth model for SWCNTs using thin-film catalysts. Understanding the growth process can lead to new insights about the growth mechanism and possibly even a method of controlling the chirality of the tubes. In spite of the amount of papers using this method, the physical phenomena of transforming a thin

[a]Author to whom correspondence should be addressed; electronic mail: rgl26@eng.cam.ac.uk
[b]The University Chemical Laboratory, Cambridge, CB2 1EW, United Kingdom.
[c]Department of Materials Science and Metallurgy, University of Cambridge, Cambridge CB2 3QZ, United Kingdom.

metal layer into nanosize particles has not been fully understood. One of the reasons for this is that more widely used techniques such as Raman, atomic force microscopy (AFM), scanning electron microscopy (SEM), or transmission electron microscopy (TEM) do not provide significant information about the layer. The fact that the thickness of the catalyst layer is very small (~1 nm) also makes it very difficult to characterize. In this situation, surface-sensitive techniques are highly advantageous. However, there has not been many studies in the literature using surface-sensitive tools such as Auger or photoemission spectroscopy. The combination of Auger spectroscopy with the spatial resolution (10 nm) of a SEM makes the Nanoauger spectroscopy a powerful technique to investigate the role of the catalyst metal layer for SWCNT growth.

The aim of this work is to study the growth process of SWCNTs from thin metal catalyst in detail by using the Nanoauger spectroscopy. How the catalyst is transformed and how it diffuses at different growth temperatures are elucidated. A surface elemental map study is also presented providing a clear view of the distribution of the catalyst on the surface. In addition, we will show how the Nanoauger spectroscopy can also be used to directly observe the single-wall carbon nanotubes.

II. EXPERIMENT

The nanotubes were grown by a thermal CVD using a 1 in. quartz tube vacuum furnace. The substrates were prepared as follows: oxidized silicon substrates are sequentially sputtered with a thin-film catalyst [Al(10 nm)/Fe(1 nm)/Mo(0.2 nm)], similar to Delzeit *et al.*,[13] in a standard rf-magnetron sputtering system. The thickness of the layers was controlled with a quartz-oscillator thickness monitor. Substrates were placed in a quartz tube that had been evacuated to 0.2 mbar and then heated to the growth temperature for 35 min and maintained there for 10 min in 500 sccm (denotes standard cubic centimeter per minute) of flowing helium at 15 mbar. After the temperature had stabilized, the helium was shut off and the tube was evacuated (<1 mbar), and a single burst of acetylene (~5 s) was introduced into the chamber. The acetylene flow rate used was 250 sccm, corresponding to a chamber pressure of 2.5 mbar. The experiment was repeated at temperatures varying from 700 to 1000 °C. These samples were investigated by a Physical Electronic PHI 680 Auger nanoprobe. An *in situ* 2 keV Ar-ion gun was also used to sputter the surface in order to provide depth-resolved chemical analysis.

III. CARBON NANOTUBE CHARACTERIZATION

Figures 1(a)–1(d) are micrographs of the nanotube growth samples prepared at different temperatures (700–1000 °C) with the same metal catalyst layers (Al/Fe/Mo). At every temperature, a single burst of acetylene (~5 s) was introduced into the chamber. It is important to note that the yield of nanotubes observed is reasonable despite the short deposition time (~5 s). As the deposition temperature increases, one observes significant changes in

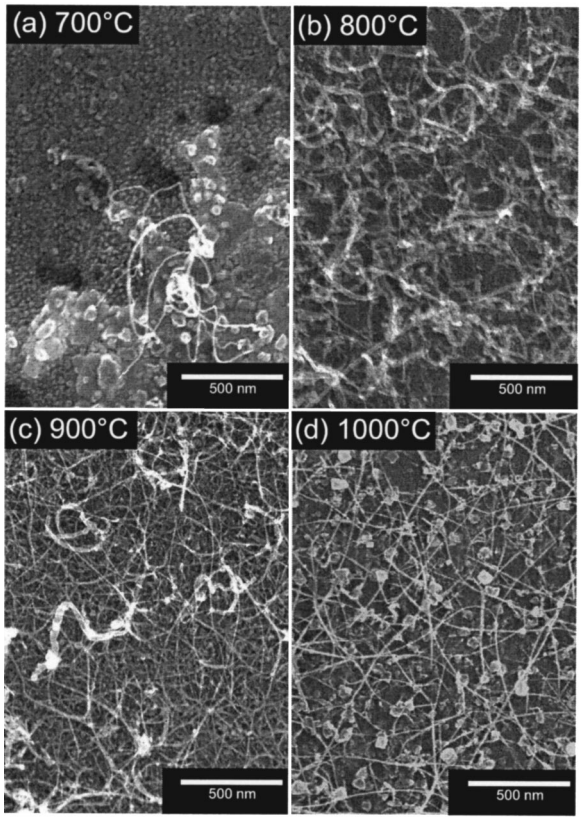

FIG. 1. Growth of carbon nanotubes using a single burst of acetylene (~5 s) at temperatures of (a) 700 °C, (b) 800 °C, (c) 900 °C, and (d) 1000 °C.

the morphology of the nanotubes produced. For every temperature, nanotubes with lengths in the range of 5–10 μm were observed, which equates to a deposition rate of about 1 and 2 μm/s. This deposition rate is similar to that found by the others.[18,19] Between 700 and 800 °C, mostly curly multiwall carbon nanotubes were found, as shown in Figs. 1(a) and 1(b). At 700 °C, the yield of nanotubes is very poor; however, at 800 °C, a dense entanglement of the curly multiwall carbon nanotubes is observed. The single-wall carbon nanotubes begin to appear at 900 °C, mixed with the other multiwall tubes [Fig. 1(c)]. 1000 °C seems to be the optimum temperature for the SWCNTs growth because very straight tubes were obtained [Fig. 1(d)]. A closer examination of Fig. 1(d) shows that the tubes are coming out of particles lying on the surface. This will be explained further in detail using the Nanoauger spectroscopy.

The presence of multiwall or single-wall tubes on the samples was first verified by the Raman spectroscopy. This technique is useful in distinguishing between the multiwall and single-wall carbon nanotubes because the spectra of SWCNTs contain particular vibrational modes. The Raman spectra in Fig. 2 show high-quality single-wall carbon nanotubes obtained for temperatures in the range between 900 and 1000 °C. The quality of the tubes can be identified using the very low ratio between the *D* (disorder) and *G* (graphitic) peaks and by noting the characteristic signature for SWCNTs, such as the *G* peak splitting and the radial breathing modes (RBM).[20,21] The RBM mode found at 183 cm^{-1}

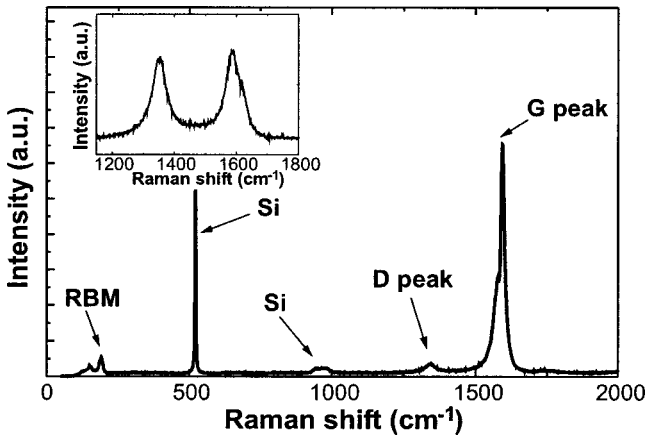

FIG. 2. Raman spectrum of the single-wall carbon nanotubes deposited at 1000 °C. The inset shows a typical Raman spectra for the multiwall carbon nanotubes deposited at lower temperatures 700–900 °C.

suggests that a great number of our SWCNTs have diameters of 1.3 nm. The inset in Fig. 2 shows the Raman spectra of the samples prepared at the lower temperatures of 700 and 800 °C. These show high-intensity *D* and *G* peaks, which is strong evidence for the presence of mostly multiwall carbon nanotubes. At temperatures around 900–950 °C, there is a transitional temperature range, and hence, nanotubes with thin diameters (1–4 nm) are obtained.

TEM also confirmed the existence of SWCNTs. The samples for TEM were prepared by depositing the triple-layer catalyst directly onto the Si_3N_4 grids and placing them into the furnace for the CVD growth. Figure 3 shows a typical TEM image of the single-wall tubes. An important observation of the TEM study is that most of the SWCNTs were found to be either isolated or to exist in bundles. Some triple-wall and double-wall nanotubes were also seen. Our TEM analysis agrees with the results reported by Li *et al.*,[22] where the carbon tubes have a closed-end cap, indicating a base-growth mechanism for CVD growth. For a better idea of the yield of the single-wall carbon nanotubes, we also performed AFM on the nanotubes grown from patterned catalyst dots 1 μm in diameter (Fig. 4). It was possible to produce on average 1–3 nanotubes of predominant diameter of 1.3 nm per catalyst dot. This is in excellent agreement with the RBM results obtained by the Raman spectroscopy and also demonstrates that the nanotubes are isolated. In these samples, the tubes are seen to emerge from small metal catalyst particles, which we have explored using the Nanoauger spectroscopy, as discussed in the next section.

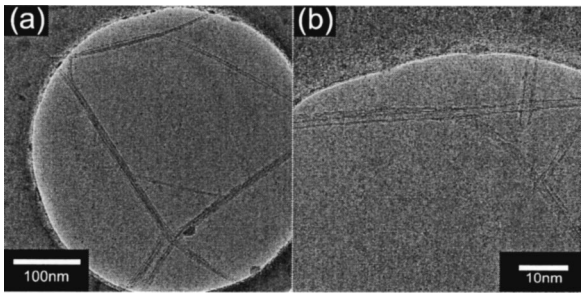

FIG. 3. Low (a) and high (b) transmission electron micrograph of SWCNTs deposited at 1000 °C.

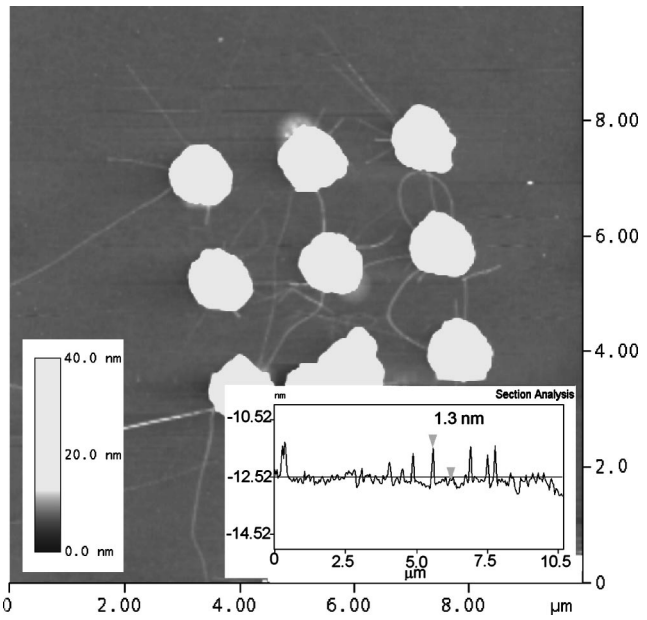

FIG. 4. (a) Atomic force microscopy (AFM) of SWCNTs coming out of the patterned dot. Inset: AFM height profile showing that most SWCNTs were found to be isolated and having a diameter of 1.3 nm.

IV. NANOAUGER SPECTROSCOPY

Figure 5(a) shows the sample surface of the as-deposited metal layers. The surface is smooth/featureless, and the elemental mapping of Al, Fe, and Mo (not shown) demonstrates a homogeneous distribution of the elements. A depth profile done by the sputtering with Ar ions is depicted in Fig.

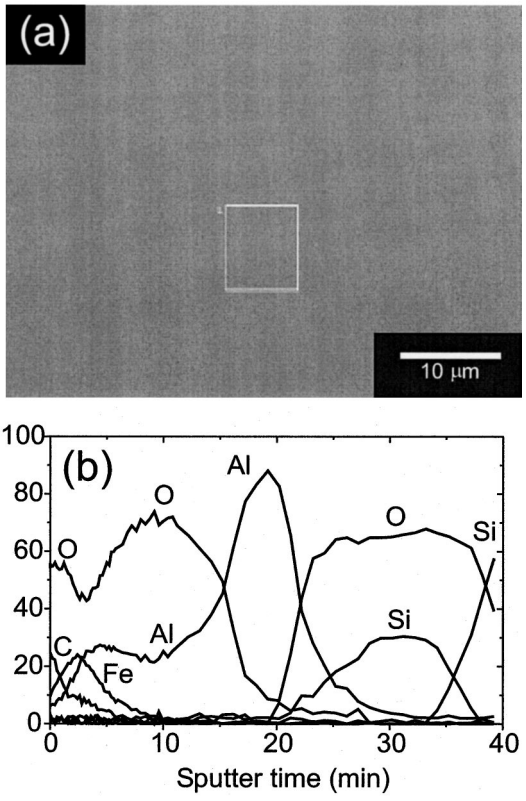

FIG. 5. (a) Scanning electron microscopy (SEM) micrograph and (b) depth profile of the as-deposited triple layer (Al+Fe+Mo).

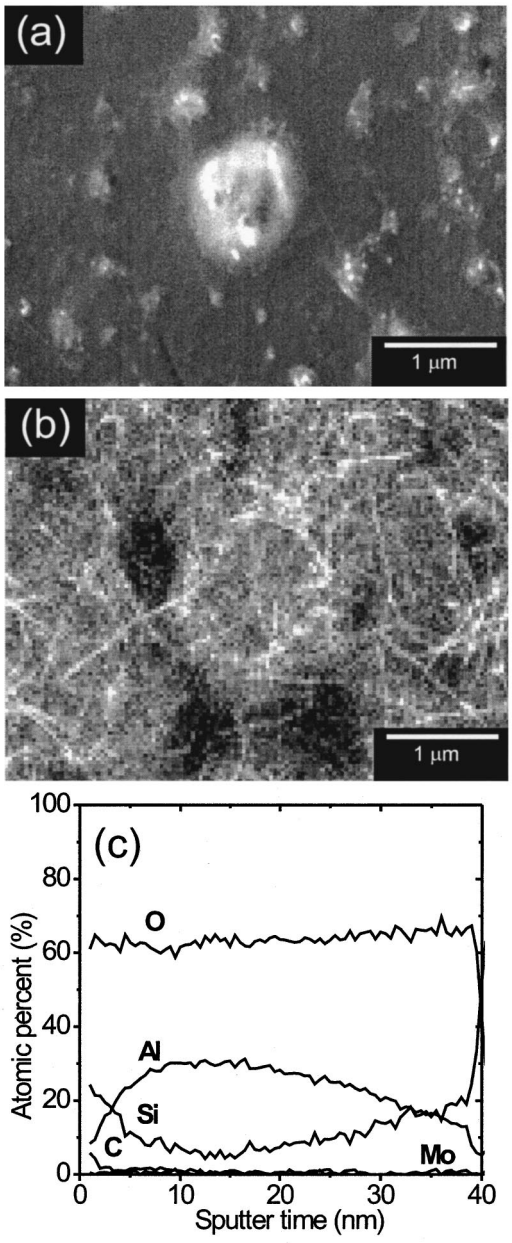

FIG. 6. (a) SEM picture of the sample deposited at 1000 °C, (b) Carbon electron Auger (KVV) map showing the single-wall nanotubes, and (c) Depth profile of the SWCNT sample deposited at 1000 °C.

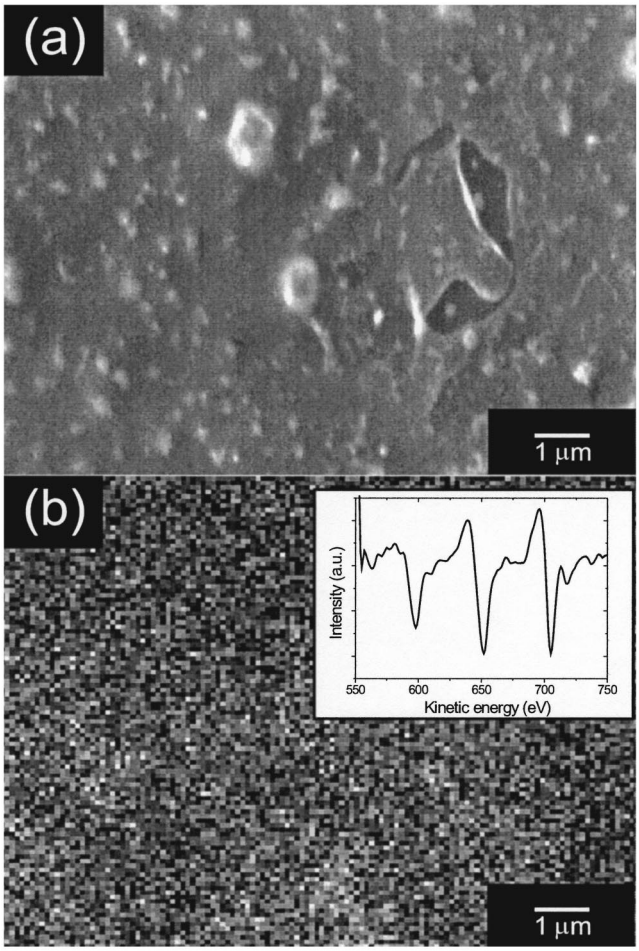

FIG. 7. (a) SEM of the sample deposited at 1000 °C and (b) 12 h map profile of Fe Auger electrons (inset: corresponding Fe Auger spectra).

5(b). It shows the presence of Fe and some carbon contamination in the outer surface. It is interesting to note that soon after the deposition, the initial 1 nm Fe layer has already been transformed into Fe oxide, which is probably due to the sample's exposure to atmosphere. Note that iron oxide particles have been extensively used in literature to produce carbon nanotubes.[7,17] With further sputtering, we observe the presence of a layer of Al oxide and pure Al. By going even further, we can finally distinguish the SiO_2 layer and the Si substrate.

Figure 6(a) shows the SEM image of the sample deposited at 1000 °C made by collecting secondary electrons in the Auger nanoprobe. Due to the relatively low resolution of the Auger microscope (15 keV), single-wall tubes could not be clearly seen using the secondary electrons. Nevertheless, we have already verified by the Raman and high-resolution SEM that there were SWCNTs on the same surface [see Fig. 1(d)]. An interesting result was obtained when carbon Auger mapping (KVV) was performed on the sample surface. Surprisingly, we were able to extract an Auger electron image of the single-wall nanotubes [Fig. 6(b)], despite being unable to evidently resolve the nanotubes when operating the Auger nanoprobe in the SEM mode. A detailed study on this result is currently underway and will be presented in the subsequent work.

Figure 6(c) depicts the depth profile of the SWCNT sample (1000 °C) after growth. The Al layer is shown to have been fully transformed into aluminium oxide (Al_xO_y). This change most likely takes place during the annealing process via the residual oxygen in the chamber. Si and Al were also detected at the surface, and their presence was probably due to the interdiffusion between the elements and the transformation of the flat Al layer into Al_xO_y particles, which reveal the underlying SiO_2. An unexpected result was the absence of a strong signal from the Fe catalyst layer. A 12-h-long acquisition of the Fe signal was then performed, which provided a clear Fe signal as well as a map profile of it on the surface. Figure 7(a) and 7(b) show the SEM picture of the area studied with a corresponding Fe map profile and an Fe Auger spectra (inset), respectively. This examination

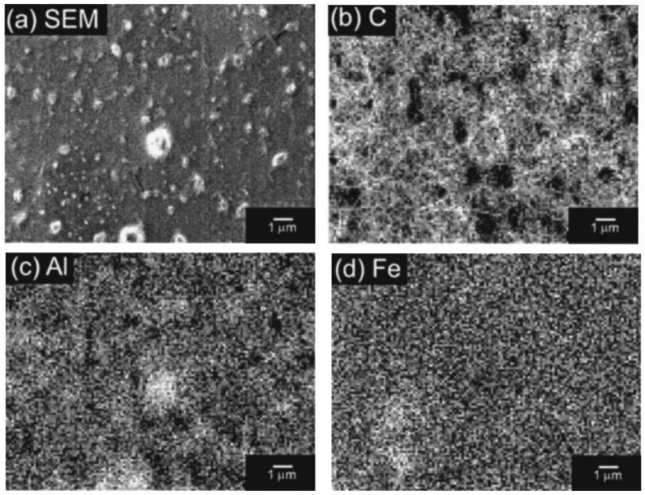

FIG. 8. (a) SEM of the probed area for the sample deposited at 1000 °C. Auger elemental map for (b) C, (c) Al, and (d) Fe.

indicates that as expected, there is Fe in the sample surface but in very small quantities, barely within the detection limit of the Auger spectroscopy. This shows that at 1000 °C, the original Fe metal layer has been transformed into particles that are very small and distributed on the surface. A similar survey of the other elements is shown in Fig. 8. Carbon mapping shows the SWCNTs. Al was detected wherever a particle of Al_xO_y was observed on the surface. These particles can be clearly seen in Fig. 1(d), and the tubes, as already mentioned, are actually coming out of these Al_xO_y particles. It is important to point out that at 1000 °C, the Fe catalyst does not seem to diffuse into the substrate as it is supported on the Al_xO_y particles.

The metal distribution is different for the samples deposited at lower temperatures (<900 °C). As already shown in Figs. 1(b) and 1(c), a dense forest of carbon tubes is obtained at deposition temperatures of 800 and 900 °C. However, at 800 °C, we produced mainly MWCNTs and a mixture of MWCNTs and SWCNTs for temperatures ranging from 900 to 950 °C. Figures 9(a)–9(f) show the SEM, C Auger electrons, and Fe Auger electrons map for temperatures of 800 and 900 °C. The first thing to note is that because there is a strong presence of MWCNTs at these temperatures, the nanotubes were easily imaged using the low-resolution SEM of the Auger microscope. We could also obtain a clear picture of the MWCNTs using the carbon Auger electrons. Conversely to what happens for the SWCNT deposition at 1000 °C, the presence of an Fe signal is very strong at these temperatures and a long acquisition time was not necessary to obtain an Fe map of the surface. We can see more localized areas of Fe that support the growth of MWCNTs; however, since the mat of carbon nanotubes is very dense, the Fe signal could be underestimated.

At 700 °C, the analysis again shows a very different result. The yield of carbon nanotubes is very low [see Fig. 1(a)], as well as poor in quality, because only fat and curly MWCNTs were obtained. Figures 10(a)–10(d) show the Auger elemental map distribution of the metals at 700 °C. The Fe has agglomerated into patchy islands, and it seems that

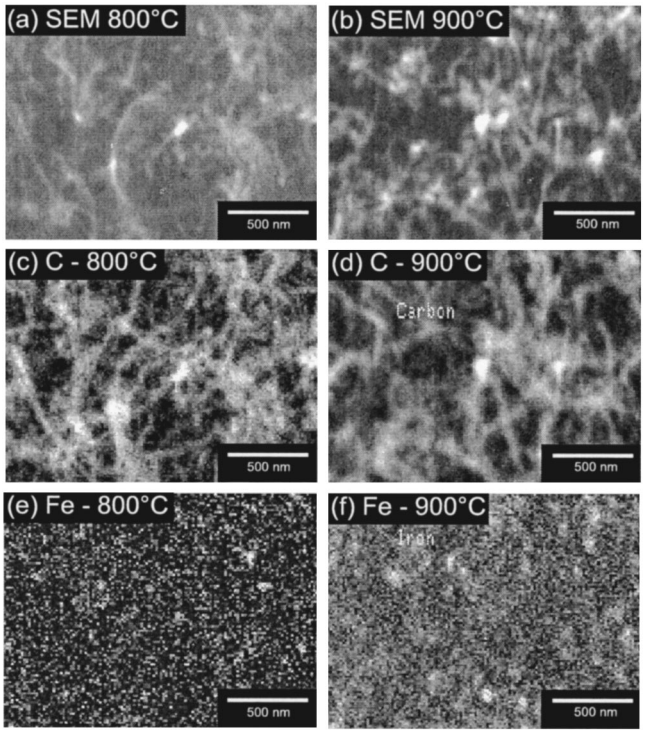

FIG. 9. (a) 800 °C and (b) 900 °C SEM picture of the MWCNTs, (c) 800 °C and (d)900 °C carbon Auger electron map picturing the nanotubes, and (e) 800 °C and (f) 900 °C analog profile of the Fe catalyst of the same area.

the curly tubes grew from these islands. This phenomenon is very similar to those observed for the growth of MWCNTs from dc plasma-enhanced chemical-vapor deposition. In this case, the metal layer sinters during the annealing to form clusters for the nanotube growth.[23] The Al, though seems to form an underlayer [Fig. 10(d)] at the surface. The Mo top layer (not shown) can barely be detected and looks homogeneously distributed along the surface. Figure 11 shows the depth profile of the triple metal layers for depositions at 700,

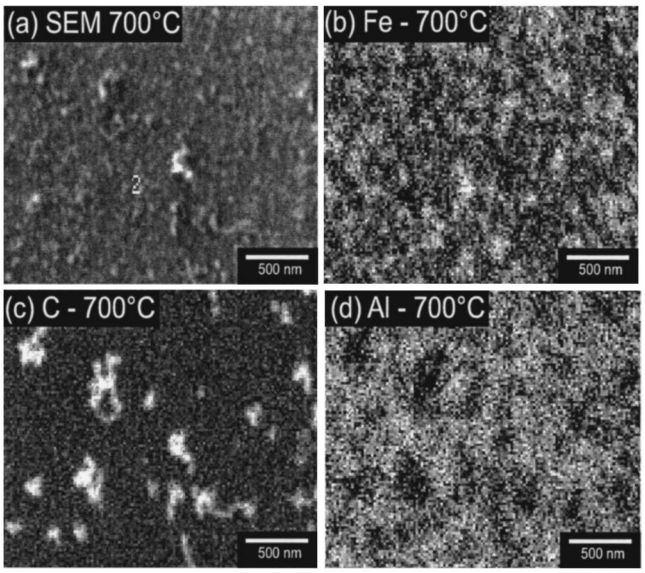

FIG. 10. (a) SEM of the sample deposited at 700 °C. Auger elemental map of (b) Fe, (c) C, and (d) Al.

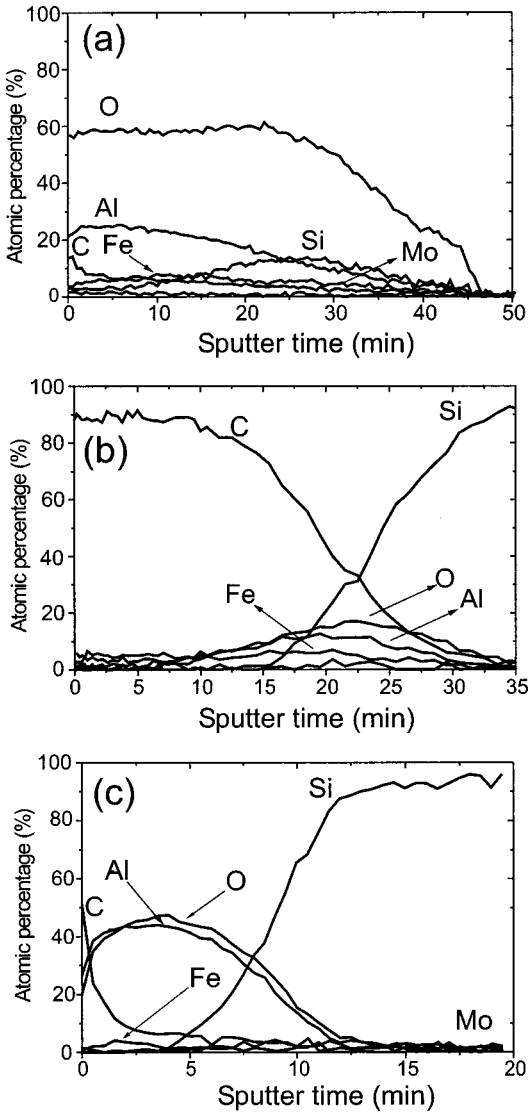

FIG. 11. Depth profile of the sample deposited at (a) 700 °C, (b) 800 °C, and (c) 900 °C.

800, and 900 °C. We can detect, in the case of the deposition at 700 °C, that there is an indication of some diffusion of the Fe catalyst layer [Fig. 11(a)]. The relatively low deposition temperature (and some Fe diffusion) could be the reason for the poor yield of nanotubes found at this temperature. At 800 and 900 °C, diffusion of the Fe could also be happening. However, in those cases, the tubes yield is very high and so a large contribution of the carbon Auger electrons is visible in the beginning of the depth profile. This is because the higher temperature (800–900 °C) provides a better clustering of the initial iron layer, resulting in a dense forest of nanotubes. It is also known that the higher the deposition temperatures, the higher is the degree of diffusion of carbon species into the catalyst, leading to a higher growth rate for CNTs. Another interesting phenomenon to be noted is the lower yield of Al_xO_y particles at lower temperatures (<900 °C). At these temperatures, large islands of Al_xO_y (Fig. 12) are sparsely observed, which is remarkably different than those of Al_xO_y particles formed at higher temperatures (~950–100 °C). Thus, the reduced deposition temperatures are probably the reason for the low efficient formation of Al_xO_y particles.

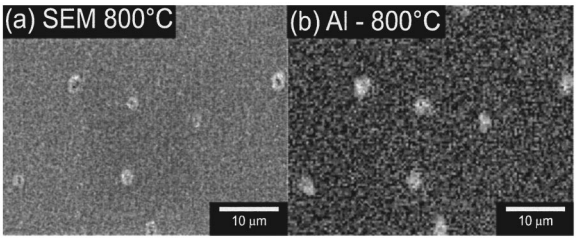

FIG. 12. (a) SEM of the sample deposited at 800 °C and (b) Al profile demonstrating the presence of Al in the islands.

V. DISCUSSION

The results presented previously are very interesting because they demonstrate that with the same initial catalyst triple layer (Al 10 nm+Fe+1 nm+Mo 0.2 nm), the growth conditions can be tuned for both the multiwall and the single-wall tubes, depending on the deposition temperature. This means that the growth temperature provides the key to the structural changes in the metal layers (in particular the Fe catalyst layer), which creates suitable conditions for the growth of the single and multiwall carbon nanotubes. In the deposition conditions used, it was found that the best temperature condition for growing SWCNTs was at 1000 °C. At this temperature, we found that the Al layer was transformed during the annealing into an Al_xO_y layer. It is known that the Al melts at temperatures around 660 °C, thus, the annealing process melts the Al and this reacts with the residual oxygen in the chamber (10^{-1} mbar base pressure) to transform it into more stable particles Al_xO_y.[24] Simultaneously, the initial Fe layer, which has been altered into iron oxide due to atmosphere exposure, is transformed into nanosized Fe particles. These Fe_xO_y nanoparticles are adsorbed onto the larger Al_xO_y particles [see Fig. 1(d)]. The physical mechanism behind the generation of pure Fe nanoparticles might be related to a reduction process, where the iron oxide loses its oxygen atom to the Si or Al underlayer.[25] Furthermore, in spite of the experimental evidence that demonstrates that a small addition of Mo increases the yield of nanotubes, the role of the Mo top layer is still not clear.[13,16] It has been suggested that the addition of Mo could help stabilize or form small Fe nanoparticles.[26,27]

A model for the growth is depicted in Fig. 13. As already mentioned previously, the initial triple layer is transformed during the annealing into Al_xO_y oxide particles. The annealing to higher temperatures also causes the essential change of

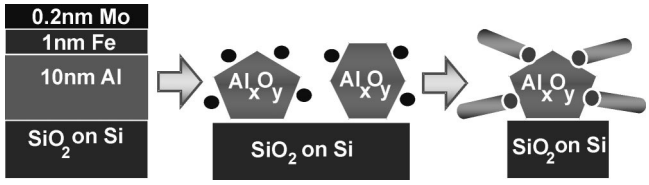

FIG. 13. Schematic model for the growth of SWCNTs using the triple metal layers.

the Fe layer into nanometer-sized Fe particles supported by the Al oxide clusters. A similar situation has been recently proposed by Zhang *et al.*[28] The fact that Fe has become distributed over the surface is thought to be the key factor in the mechanism for the growth of the single-wall carbon nanotubes at higher temperatures (900–1000 °C). This result is supported by the difficulty in detecting Fe by a surface-sensitive technique such as Auger spectroscopy. No apparent diffusion was observed at this temperature, so the Al_xO_y underlayer plays the key role of providing the proper stable support for the Fe nanoparticles to interact with the carbon source (see Fig. 13). In other words, the formation of the Al_xO_y clusters together with the formation of very small Fe nanoparticles are the critical factors for the formation of SWCNTs. It is important to keep in mind that the growth of carbon nanotubes is a thermally activated process, so higher temperatures provide more energy for the diffusion of the carbon into the catalyst and the subsequent growth of the nanotubes. Therefore, we note two important factors for the growth to be considered: (1) the reorganization of the initial Fe layer into particles and (2) the deposition temperature. At lower temperatures (<900 °C), the Al oxide layer does not transform completely into Al_xO_y particles, in addition to some diffusion of the Fe. As a consequence, Fe does not transform into nanosized particles at lower temperatures but rather agglomerates into large islands, providing then a high yield of larger diameter multiwall tubes (10–30 nm in diameter).

VI. CONCLUSION

A careful study of the growth of the multiwall and single-wall carbon nanotubes using a thin-film triple layer as the catalyst is presented. At lower deposition temperatures (<900 °C), MWCNTs were obtained, whereas at higher temperatures (~1000 °C), high-quality SWCNTs were produced. The growth was performed by a single and a short burst of acetylene gas (~5 s) under vacuum conditions. The transformation of the initial metal layers was monitored by an Auger elemental mapping of the sample surface. At 1000 °C, the formation of Al_xO_y particles and the sintering of the Fe layer into nanosized particles was observed. Nanosize Fe particles are then adsorbed among the Al_xO_y particles. At lower temperatures, there is a less effective generation of Al_xO_y clusters and the Fe catalyst reorganizes itself into larger islands (resulting in the MWCNTs growth). The combining effect from the formation of Al_xO_y particles and the complete change of the Fe layer into small particles provides the optimum environment for the SWCNT growth.

ACKNOWLEDGMENTS

The authors would like to acknowledge the support they received from the EPSRC CBE program and CANVAD project funded by EC. Two of the authors (K.B.K.T. and R.G.L.) also acknowledge the support of Christ's College and Wolfson College, respectively. Thomas Swan Nano Instruments is acknowledged for the support in equipment development. The authors would also like to thank Dr. D. G. Hasko for the use of microelectronics facilities, Dr. M. S. M. Saifullah, and Dr. D. J. Kang for the focus ion-beam process.

[1] *Carbon Nanotubes: Synthesis, Structure, Properties, and Applications*, edited by M. S. Dresselhaus G. Dresselhaus, and P. Avouris (Springer, New York, 2001).
[2] A. Thess *et al.*, Science **273**, 483 (1996).
[3] C. Journet *et al.*, Nature (London) **388**, 756 (1997).
[4] N. R. Franklin and H. J. Dai, Adv. Mater. (Weinheim, Ger.) **12**, 12 (2000).
[5] N. R. Franklin, Q. Wang, T. W. Tombler, A. Javey, M. Shim, and H. Dai, Appl. Phys. Lett. **81**, 913 (2002).
[6] Y. Homma, Y. Kobayashi, T. Ogino, and T. Yamashita, Appl. Phys. Lett. **81**, 2261 (2002).
[7] J. Kong, A. M. Cassell, and H. Dai, Chem. Phys. Lett. **292**, 567 (1998).
[8] J. H. Hafner, M. J. Bronikowski, B. R. Azamian, P. Nikolaev, A. G. Rinzler, D. T. Colbert, K. A. Smith, and R. E. Smalley, Chem. Phys. Lett. **296**, 195 (1998).
[9] R. G. Lacerda *et al.*, Appl. Phys. Lett. **84**, 269 (2004).
[10] H. C. Choi, W. Kim, D. Wang, and H. Dai, J. Phys. Chem. B **106**, 12631 (2002).
[11] Y. Li, W. Kim, Y. Zhang, M. Rolandi, D. Wang, and H. Dai, J. Phys. Chem. B **105**, 11424 (2001).
[12] C. L. Cheung, A. Kurtz, H. Park, and C. M. Lieber, J. Phys. Chem. B **106**, 2429 (2002).
[13] L. Delzeit, B. Chen, A. Cassell, R. Stevens, C. Nguyen, and M. Meyyappan, Chem. Phys. Lett. **348**, 368 (2001).
[14] L. Marty, V. Bouchiat, A. M. Bonnot, M. Chaumont, T. Fournier, S. Decossas, and S. Roche, Microelectron. Eng. **61–62**, 485 (2002).
[15] R. Seidel, M. Liebau, G. S. Duesberg, F. Kreupl, E. Unger, A. P. Graham, W. Hoenlein, and W. Pompe, Nano Lett. **3**, 965 (2003).
[16] J. W. Ward, B. Q. Wei, and P. M. Ajayan, Chem. Phys. Lett. **376**, 717 (2003).
[17] Y. J. Jung, Y. Homma, T. Ogino, Y. Kobayashi, D. Takagi, B. Wei, R. Vajtai, and P. M. Ajayan, J. Phys. Chem. B **107**, 6859 (2003).
[18] W. Kim, H. C. Choi, M. Shim, Y. Li, D. Wang, and H. Dai, Nano Lett. **2**, 703 (2002).
[19] S. Huang, X. Cai, and J. Liu, J. Am. Chem. Soc. **125**, 5636 (2003).
[20] A. Jorio, R. Saito, J. H. Hafner, C. M. Lieber, M. Hunter, T. McClure, G. Dresselhaus, and M. S. Dresselhaus, Phys. Rev. Lett. **86**, 1118 (2001).
[21] M. S. Dresselhaus, A. Jorio, A. G. Souza, G. Dresselhaus, and R. Saito, Physica B **323**, 15 (2002).
[22] Y. Li, Y. Zhang, M. Roland, D. Wang, and H. Dai, J. Phys. Chem. B **105**, 11424 (2001).
[23] M. Chhowalla *et al.*, J. Appl. Phys. **90**, 5308 (2001).
[24] T. de Los Arcos, Z. M. Wu, and P. Oelhafen, Chem. Phys. Lett. **380**, 419 (2003).
[25] K. Prabhakaran, K. V. P. M. Shafi, A. Ulman, P. M. Ajayan, Y. Homma, and T. Ogino, Surf. Sci. Lett. **506**, L250 (2002).
[26] J. E. Herrara, L. Balzano, A. Borgna, W. E. Alvarez, and D. E. Resasco, J. Catal. **204**, 129 (2001).
[27] Y. J. Yoon, J. C. Bae, H. K. Baik, S. J. Cho, S. Lee, K. M. Song, and N. S. Myung, Chem. Phys. Lett. **366**, 109 (2002).
[28] R. Y. Zhang, I. Amlani, J. Baker, J. Tresek, R. K. Tsui, and P. Fejes, Nano Lett. **3**, 731 (2003).